

# Combination of Multiple Global Descriptors for Image Retrieval

HeeJae Jun\*    Byungsoo Ko\*    Youngjoon Kim    Insik Kim    Jongtack Kim  
NAVER/LINE Vision

{heejae.jun, byungsoo.ko, kim.youngjoon, insik.kim, jongtack.kim}@navercorp.com

## Abstract

Recent studies in image retrieval task have shown that ensembling different models and combining multiple global descriptors lead to performance improvement. However, training different models for the ensemble is not only difficult but also inefficient with respect to time and memory. In this paper, we propose a novel framework that exploits multiple global descriptors to get an ensemble effect while it can be trained in an end-to-end manner. The proposed framework is flexible and expandable by the global descriptor, CNN backbone, loss, and dataset. Moreover, we investigate the effectiveness of combining multiple global descriptors with quantitative and qualitative analysis. Our extensive experiments show that the combined descriptor outperforms a single global descriptor, as it can utilize different types of feature properties. In the benchmark evaluation, the proposed framework achieves the state-of-the-art performance on the CARS196, CUB200-2011, In-shop Clothes, and Stanford Online Products on image retrieval tasks. Our model implementations and pretrained models are publicly available<sup>1</sup>.

## 1. Introduction

Since the ground-breaking in 2012 ImageNet competition [10, 27], image descriptors based on deep convolutional neural networks (CNNs) have surfaced as generic descriptors in computer vision tasks, including classification [27, 17, 51], object detection [12, 45, 44], and semantic segmentation [33, 7, 46]. Moreover, recent works leveraging image descriptors based on deep CNNs have emerged for image retrieval task which used to apply conventional methods relying on local descriptor matching [34, 23] and re-ranking with spatial verification [36, 52, 29].

In the case of recent researches on image retrieval [4, 13], fully connected (FC) layers after several convolutional layers are used as global descriptors followed by dimensionality reduction. Other works generate global descriptors from

the activations of the convolutional layers. Representative global descriptors generated by global-pooling methods include sum pooling of convolutions (SPoC) [3], maximum activation of convolutions (MAC) [53], and generalized-mean pooling (GeM) [43]. The performance of each global descriptor varies by dataset as each descriptor has different properties [5]. For example, SPoC activates larger regions on the image representation while MAC activates more focused regions [19].

Recent researches have focused on ensemble techniques for image retrieval task. Conventional ensemble techniques which train multiple learners individually and use a combined model lead to an increase in performance [31, 58, 41, 24]. Many high-ranked approaches [42, 6] in the recent Google landmark retrieval challenge [2] and Zehang *et al.* [31] boost the performance by combining different global descriptors which are trained individually. However, explicitly training multiple learners for ensemble could lead to longer training time and higher memory consumption. In order to handle this problem, other ensemble approaches [24, 41] attempt to train a retrieval model in an end-to-end manner. These approaches can be tricky as they need specifically designed strategy or loss to control diversity among learners, which also cause a more laborious training process.

In this paper, we focus on how to exploit multiple global descriptors to get an ensemble effect without explicitly training multiple learners and controlling diversity among learners. Our contribution is threefold. (1) We propose a novel framework, the combination of multiple global descriptors (CGD), that combines multiple global descriptors which can be trained in an end-to-end manner. It achieves an ensemble effect without any explicit ensemble model or diversity control over each global descriptor. Moreover, the proposed framework is flexible and expandable by the global descriptor, CNN backbone, loss, and dataset. To the best of our knowledge, we are the first to leverage multiple types of global descriptors to get a final descriptor in the image retrieval task. (2) We investigate the effect of combining multiple global descriptors with quantitative and qualitative analysis. Our extensive experiments demonstrate that

\* Authors contributed equally

<sup>1</sup><https://github.com/naver/cgd>

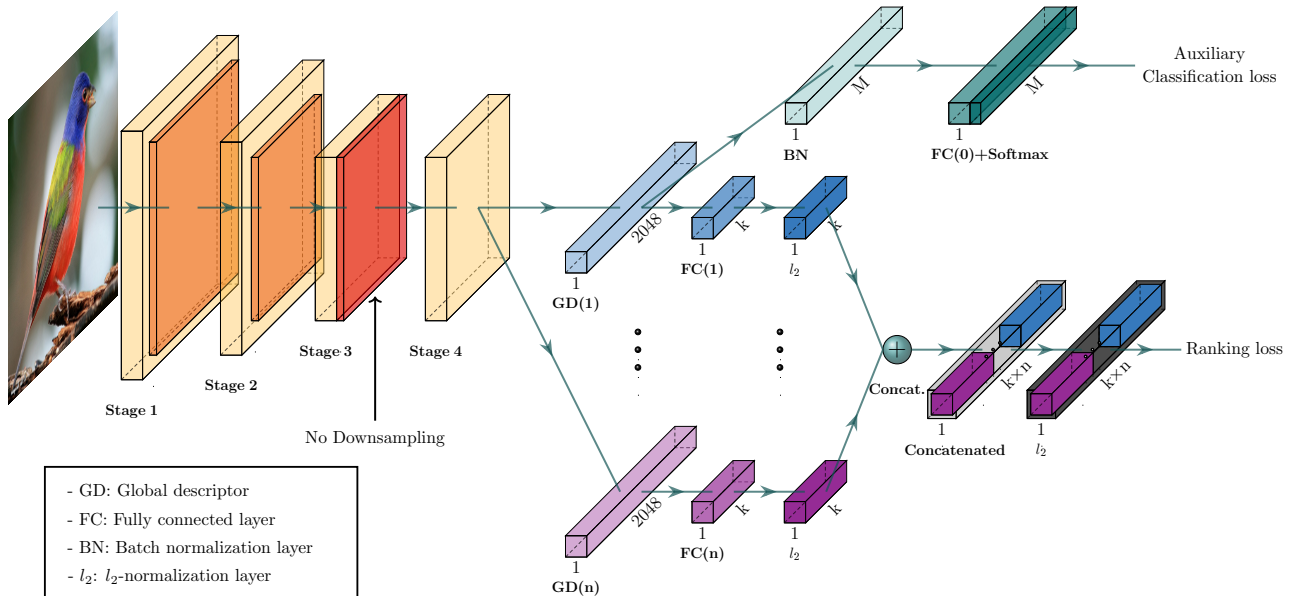


Figure 1. The combination of multiple global descriptors (CGD) framework. The framework is described with ResNet-50 backbone where Stage 3 downsampling is removed. From the last feature map, each of  $n$  global descriptor branch outputs a  $k$ -dimensional embedding vector, which is concatenated into the combined descriptor for ranking loss. Exclusively the first global descriptor is used for auxiliary classification loss where  $M$  denotes the number of classes.

using combined descriptor outperforms a single global descriptor because it can use different types of feature properties. (3) The proposed framework achieves the state-of-the-art performance on CARS196 [26], CUB200-2011 [54] (CUB200), Stanford Online Products [39] (SOP) and In-shop Clothes [32] (In-shop) by a large margin on image retrieval tasks.

## 2. Related Works

In the recent works for image retrieval task, global descriptors based on deep CNNs have been used as off-the-shelf feature [47, 3] over the conventional hand-crafted features such as SIFT [34]. SPoC [3] is sum pooling from the feature map which performs well mainly due to the subsequent descriptor whitening. MAC [53] by max pooling is another powerful descriptor, while regional MAC [53] performs max pooling over regions, then sum over the regional MAC descriptors at the end. GeM [43] generalizes max and average pooling with a pooling parameter. Other global descriptor method includes weighted sum pooling [22], weighted GeM [57], multiscale RMAC [30], etc.

Some works [9, 15, 28] attempt using the additional strategy or the attention mechanism to maximize the activations of essential features on the feature map. Dai *et al.* [9] present a strategy called batch feature erasing (BFE) to force the network to optimize the feature representation of different regions. Li *et al.* [28] propose a model that has soft pixel attention and hard regional attention along with simultaneous optimization of feature representations. The

downsides of adopting the additional strategy or the attention mechanism are that it can not only lead to an increase network size and training time, but also require additional parameters for training. However, our proposed framework does not need any additional strategy or attention mechanism when it requires only a few additional parameters for training.

The ensemble is a well-known technique that aims to boost performance by training multiple learners and obtains a combined result from the trained learners. In the last decades, it is widely used in image retrieval tasks [24, 41, 58, 31]. Xuan *et al.* [58] propose a method where each embedding function is learned by randomly bagging and training labels into small subsets. Kim *et al.* [24] suggest an attention-based ensemble, where single feature embedding function is trained while each learner learns different attention modules. The downside of ensemble techniques is that it leads to an increase in computational cost as the model complexity increases [62], and requires additional control to yield diversity between learners [24, 40]. However, our proposed framework takes advantage of the idea of the ensemble technique when it can be trained in an end-to-end manner with no diversity control.

## 3. Proposed Framework

We propose a simple, yet effective framework which we refer to as a CGD framework for image retrieval tasks. It learns a combined descriptor which is generated by concatenating multiple global descriptors in an end-to-end manner.

Our proposed framework is depicted in Figure 1.

The proposed framework consists of a CNN backbone network and two modules. The first module is the main module that learns an image representation, which is a combination of multiple global descriptors for a ranking loss. Next, is an auxiliary module to fine-tune a CNN with a classification loss. The proposed framework is trained with a final loss, which is the sum of the ranking loss from the main module and the classification loss from the auxiliary module in an end-to-end manner.

### 3.1. Backbone Network

Our proposed framework can use any CNN backbones such as BN-Inception [21], ShuffleNet-v2 [35], ResNet [17] and its variants, etc, while we use ResNet-50 [17] as a baseline backbone described in Figure 1. To preserve more information in the last feature map, we modify the network by discarding the down-sampling operation between Stage 3 and Stage 4 [9, 55]. This modification gives a  $14 \times 14$  sized feature map at the end for input size of  $224 \times 224$ , which improves the performance by containing richer information.

### 3.2. Main Module: Multiple Global Descriptors

The main module has multiple branches that output each image representation by using different global descriptors on the last convolutional layer. In this paper, we use three types of the most representative global descriptors on each branch, including SPoC, MAC, and GeM.

Given an image  $I$ , the output of the last convolutional layer is a 3D tensor  $\mathcal{X}$  of  $C \times H \times W$  dimension, where  $C$  is the number of feature maps. Let  $\mathcal{X}_c$  be the set of  $H \times W$  activations for feature maps  $c \in \{1 \dots C\}$ . The network output consists of  $C$  channels of such 2D feature maps. Global descriptor takes  $\mathcal{X}$  as input and produces a vector  $f$  as output by pooling process. Such pooling methods can be generalized as follows:

$$f = [f_1 \dots f_c \dots f_C]^\top, \quad f_c = \left( \frac{1}{|\mathcal{X}_c|} \sum_{x \in \mathcal{X}_c} x^{p_c} \right)^{\frac{1}{p_c}}. \quad (1)$$

We define SPoC as  $f^{(s)}$  when  $p_c = 1$ , MAC as  $f^{(m)}$  when  $p_c \rightarrow \infty$ , and GeM as  $f^{(g)}$  for the rest of the cases. For the case of GeM, the parameter  $p_c$  can be manually set or trained because it is differentiable, while we use fixed  $p_c$  parameter 3 throughout the experiments.

Output feature vector  $\Phi^{(a_i)}$  from the  $i$ -th branch is generated by dimensionality reduction through the FC layer and normalization through the  $l_2$ -normalization layer:

$$\Phi^{(a_i)} = \frac{W^{(i)} \cdot f^{(a_i)}}{\|W^{(i)} \cdot f^{(a_i)}\|_2}, \quad a_i \in \{s, m, g\}, \quad (2)$$

for  $i \in \{1 \dots n\}$ , where  $n$  is the number of branches,  $W^i$  is the weight of the FC layer and the global descriptor  $f^{(a_i)}$

can be SPoC when  $a_i = s$ , MAC when  $a_i = m$ , or GeM for  $a_i = g$ .

The final feature vector referred to as combined descriptor  $\psi_{CGD}$  of our framework combines output feature vectors of multiple branches and performs  $l_2$ -normalization sequentially:

$$\psi_{CGD} = \frac{\Phi^{(a_1)} \oplus \dots \oplus \Phi^{(a_i)} \oplus \dots \oplus \Phi^{(a_n)}}{\|\Phi^{(a_1)} \oplus \dots \oplus \Phi^{(a_i)} \oplus \dots \oplus \Phi^{(a_n)}\|_2}, \quad (3)$$

for  $a_i \in \{s, m, g\}$ , where  $\oplus$  denotes concatenation. This combined descriptor can be trained with any ranking loss, while we use batch-hard triplet loss [18] as a representative.

In the proposed framework, there are two advantages to combining multiple global descriptors. First, it gives an ensemble effect with only a few additional parameters. To get the ensemble effect while making it trainable in an end-to-end manner, our framework extracts and combines multiple global descriptors within a single CNN backbone. Second, it automatically provides different properties for each branch's output without any diversity control. While [24, 40] propose specially designed losses to encourage diversity among learners, our framework does not require any specially designed loss to control diversity among branches.

### 3.3. Auxiliary Module: Classification Loss

The auxiliary module fine-tunes the CNN backbone based on the first global descriptor of the main module by using a classification loss. It is motivated by the approach [14], which consists of two steps: training a CNN backbone with a classification loss and then fine-tuning the network with a triplet loss. However, we refine their approach to have a single step for end-to-end training, while [14] has to be trained with two steps. Training with auxiliary classification loss helps to maximize inter-class distance which makes the model to train faster and stable.

Temperature scaling [16, 61] in softmax cross-entropy loss (softmax loss), and label smoothing [51] are proven to be helpful for the training process. The softmax loss is defined as

$$L_{Softmax} = -\frac{1}{N} \sum_{i=1}^N \log \frac{\exp((W_{y_i}^T f_i + b_{y_i})/\tau)}{\sum_{j=1}^M \exp((W_j^T f_i + b_j)/\tau)}, \quad (4)$$

where  $N$ ,  $M$ , and  $y_i$  are the batch size, the number of classes, and the corresponding identity label of  $i$ -th input, respectively.  $W$ , and  $b$  are trainable weight, and bias, respectively.  $f$  is a global descriptor from the first branch, where  $\tau$  is a temperature parameter with default value 1. The temperature scaling with low-temperature parameter  $\tau$  in the Equation 4, assigns a larger gradient to more challenging examples and is helpful for intra-class compact, and inter-class spread-out embedding. The label smoothing enhances a model, thereby improves generalization by

estimating the marginalized effect of a label-dropout during training. Therefore, to prevent over-fitting, and learn better embedding, we add label smoothing and temperature scaling in the auxiliary classification loss.

### 3.4. Configurations of Framework

**Configurations** Our proposed framework is expandable by the number of global descriptor branches, and it allows different types of networks according to the configuration of global descriptors. As we use SPoC (S), MAC (M), GeM (G), and exclusively the first global descriptor is used for the auxiliary classification loss, we can make twelve possible configurations. First letter in a notation is the first global descriptor to be used for the auxiliary classification loss. For example with a configuration SMG, the first letter which is the first global descriptor S will be used for the auxiliary classification loss and all S, M, and G are concatenated to be combined descriptor for ranking loss. Therefore, the twelve configurations are obtained as follows: S, M, G, SM, MS, SG, GS, MG, GM, SMG, MSG, GSM.

**How to Choose the Best** As each global descriptor has different properties, the performance of each descriptor can vary by datasets [5]. In order to find the best configuration, we evaluate every single descriptor and choose the highest and the second-highest single descriptors to use them for combination. The number of global descriptors to combine has to be determined by the size of output dimensionality. For a small output dimensionality, a small number of descriptors is recommended. This rule to choose the best configuration is shown with an experiment below in Section 4.4.1.

### 3.5. Efficiency of Time and Memory

Compared to previous methods of feature ensemble [42, 6, 31], our proposed framework has better efficiency in terms of time and memory. Because each learner of an ensemble method needs individual training and inference, ensembling  $N$  number of learners with different global descriptors requires  $N$  number of GPUs, and it requires post-processing step such as concatenation or normalization. Our proposed method needs only one GPU independently of the number of global descriptors without any post-processing step because of a shared backbone. Given limited memory resources, training and inference of a model in an end-to-end manner is beneficial in terms of time and memory.

## 4. Experiments

### 4.1. Datasets

We evaluate our proposed framework on image retrieval datasets including CUB200-2011 [54], CARS196 [26], Stanford Online Products [39], and In-shop Clothes [32].

Loss	Recall@K (%)			
	1	2	4	8
Rank	86.7 ± 0.3	92.1 ± 0.3	95.3 ± 0.2	97.3 ± 0.1
Both	<b>93.1 ± 0.1</b>	<b>96.0 ± 0.2</b>	<b>97.4 ± 0.2</b>	<b>98.3 ± 0.2</b>

Table 1. Recall@K ± std. dev. comparison between using only the ranking loss (Rank) and using both the classification and ranking losses (Both) on CARS196. We report results over five runs.

Trick	Recall@K (%)			
	1	2	4	8
None	93.1 ± 0.1	96.0 ± 0.2	97.4 ± 0.2	98.3 ± 0.2
LS	93.5 ± 0.2	96.1 ± 0.1	97.5 ± 0.1	98.4 ± 0.1
TS	94.0 ± 0.1	96.4 ± 0.2	97.8 ± 0.1	98.7 ± 0.1
Both	<b>94.4 ± 0.2</b>	<b>96.8 ± 0.0</b>	<b>98.0 ± 0.0</b>	<b>98.8 ± 0.1</b>

Table 2. Recall@K ± std. dev. among the baseline ‘no tricks’ (None), label smoothing (LS), temperature scaling (TS), and ‘both tricks’ (Both) on CARS196. We report results over five runs.

For CUB200 and CARS196, cropped images with bounding box information are used. We follow the same training and test split as [9, 24, 60] for fair comparisons.

### 4.2. Implementation

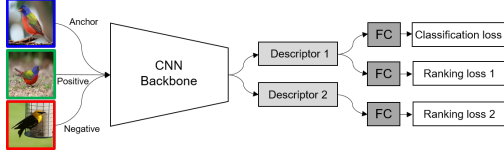
All experiments are implemented using MXNet [8] on a Tesla P40 GPU with 24 GB memory. We use BN-Inception [21], ShuffleNet-v2 [35], ResNet-50 [17], SE-ResNet-50 [20] with ImageNet ILSVRC-2012 [10] pre-trained weights from MXNet GluonCV [1]. For every experiment, we use the input size of  $224 \times 224$  and the 1536-dimensional embedding, unless otherwise noted in the experiment. In the training phase, the input image is resized to  $252 \times 252$ , cropped randomly to  $224 \times 224$ , and then flipped randomly to the horizontal. We use an Adam [25] optimizer with a learning rate of  $1e-4$ , and a step decay is used for scheduling the learning rate. A margin of  $m$  for triplet loss is 0.1, and a temperature of  $\tau$  for softmax loss is 0.5, with a batch size of 128 for every experiment. In the inference phase, we only resize the image by the default input size of  $224 \times 224$ .

### 4.3. Experiments for Architecture Design

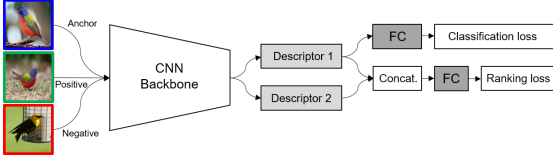
#### 4.3.1 Training Classification and Ranking Loss Jointly

**Auxiliary Classification Loss** Our proposed framework is trained by a ranking loss with an auxiliary classification loss from a descriptor of the first branch. We compare the performance between using the ranking loss exclusively, and the ranking loss with the auxiliary classification loss on CARS196 in the Table 1. In this experiment, we do not apply label smoothing, and temperature scaling on the auxiliary classification loss in every case. It shows that using both losses provides higher performance than using ranking loss exclusively. Classification loss focuses on cluster-





(a) Architecture type A.



(b) Architecture type B.

Figure 2. Different architecture types for training multiple global descriptors.

ing each class into a close embedding space on a categorical level. Ranking loss focuses on gathering samples in the same class and making a distance between samples from the different classes in the instance level. Therefore, training the ranking loss with the auxiliary classification loss jointly gives better optimization for categorical, and fine-grained feature embedding.

**Label Smoothing and Temperature Scaling** As mentioned in Section 3.3, label smoothing, and temperature scaling are proven to be helpful to learn better embedding for the classification loss. We investigate if it can be applied when a model is trained with both the ranking loss and the auxiliary classification loss. We show the performance appraisal of the ‘no tricks’, the label smoothing, the temperature scaling with temperature term 0.5, and ‘both tricks’ on the auxiliary classification loss in Table 2. The experiment is performed on the ResNet-50 [17] backbone with the configuration SM. It shows that each label smoothing and temperature scaling improves the performance compared to the ‘no tricks’. Moreover, applying ‘both tricks’ together stacks up each performance boost, and gives the best performance.

### 4.3.2 Combining Multiple Global Descriptors

**Position of Combination** As our proposed framework uses multiple global descriptors, we perform experiments with different positions of a combination of multiple global descriptors to choose the best architecture. Architecture type A in the Figure 2a trains each global descriptor with individual ranking loss, and then combines them at the inference phase as in [24], while they use the same global descriptor for every branch and do not use classification loss. Architecture type B in the Figure 2b combines the raw output of global descriptors and train it with a single ranking loss, similar to studies of [48, 50], while they do not use multiple global descriptors. Also, our proposed framework

Type	Recall@K (%)			
	1	2	4	8
A	74.6 ± 0.4	83.5 ± 0.4	89.8 ± 0.3	<b>94.0 ± 0.2</b>
B	73.7 ± 0.3	82.6 ± 0.3	89.2 ± 0.2	93.5 ± 0.2
CGD	<b>75.3 ± 0.5</b>	<b>83.9 ± 0.3</b>	<b>89.9 ± 0.3</b>	<b>94.0 ± 0.3</b>

Table 3. Recall@K ± std. dev. among architecture type A, type B, and the proposed framework with the configuration SM on CUB200-2011. We report results over five runs.

Comb.	Recall@K (%)			
	1	2	4	8
Sum	73.8 ± 0.5	82.9 ± 0.4	89.4 ± 0.3	93.7 ± 0.1
Concat	<b>75.3 ± 0.5</b>	<b>83.9 ± 0.3</b>	<b>89.9 ± 0.3</b>	<b>94.0 ± 0.3</b>

Table 4. Recall@K ± std. dev. comparison by combination method with the configuration SM on CUB200-2011. We report results over five runs.

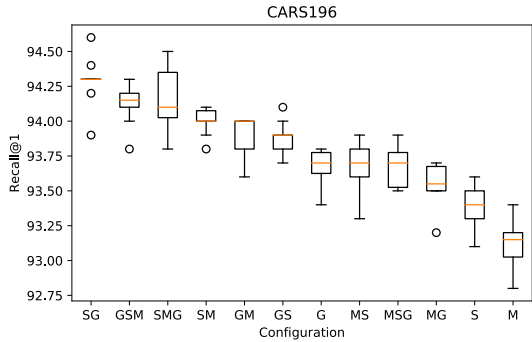
combines multiple global descriptors after the FC layers and  $l_2$ -normalization as described in Figure 1. As shown in Table 3, the proposed position of the combination presents the best performance over the architecture type A and type B. The reason is that CGD can maintain properties and diversities of each feature vector from multiple branches. In contrast, the final embedding of type A in the training phase is different from that of the inference phase, and the final embedding of type B loses each property of the global descriptors because they are mixed up by FC layer after concatenation.

**Method of Combination** In terms of the combination method, concatenation, and summation of multiple descriptors are proven to enhance performance in [24, 48, 50, 53, 9]. Therefore, we compare two combination methods to choose the best. As shown in Table 4, concatenation of multiple global descriptors gives better performance compared to their summation. This also indicates the importance of preserving each property, and diversity from multiple global descriptors, as the summation mix activations of each global descriptor up, while the concatenation maintains them.

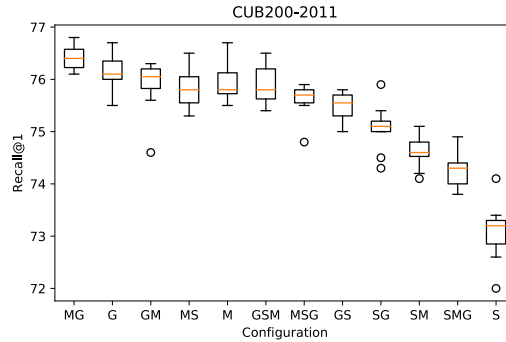
## 4.4. Effectiveness of Combined Descriptor

### 4.4.1 Quantitative Analysis

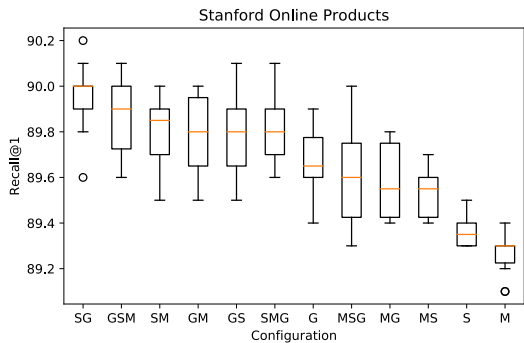
The core of our proposed framework is exploiting multiple global descriptors. As we defined in Section 3.4, we conduct experiments with twelve possible configurations on each image retrieval dataset. In the Figure 3, majorities of combined descriptors outperform over than single global descriptors. Moreover, the best configuration is a combination of the highest and the second-highest single descriptors, which we will use this pattern to find the best configuration, as mentioned in Section 3.4. While the performance of each descriptor is varied by the properties of datasets, the main



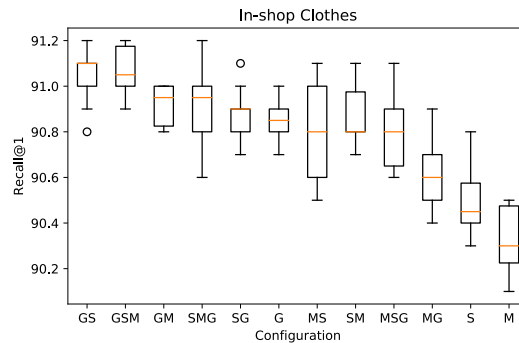
(a) Recall@1 (%) on CARS196.



(b) Recall@1 (%) on CUB200-2011.



(c) Recall@1 (%) on Stanford Online Products.



(d) Recall@1 (%) on In-shop Clothes.

Figure 3. Performance of different configurations of our proposed framework. For the faster experiments on SOP, we use a mini-test set by sampling a hundred instances per class. Due to the uncertainty of deep learning model, we report results over ten runs with box plots.

essence is that exploiting multiple global descriptors gives performance boost compared to single global descriptors.

Table 5 shows the performance of individual global descriptors before combining operation and how much performance gain they can produce after the operation. Every combined descriptor have 1536-dimensional embedding vector, while individual descriptor has 1536-dimensional embedding vector for S, M, G, 768-dimensional embedding vector for SM, MS, SG, GS, MG, GM, and 512-dimensional embedding vector for SMG, MSG, GSM. Having a larger embedding dimension usually gives better performances. However, if the performance difference is not much between a large embedding and a small embedding, it may be preferable to use multiple small embeddings from different global descriptors. For example, as individual descriptor GeM from SG with 768 embedding dimensions has similar performance with a single descriptor G with 1536 embedding dimensions, SG gets a significant performance boost by combining different features of SPoC, and GeM.

#### 4.4.2 Qualitative Analysis

A visualization tool proposed in [49] highlights the regions of images that contribute the most to pairwise similarity. We modify this work for our framework to see how much each

Config.	Combined (1536-dim.)	Individual Descriptor			
		SPoC	MAC	GeM	Dim.
S	-	<b>93.8</b>	-	-	1536
M	-	-	93.6	-	
G	-	-	-	93.9	
SM	94.3	92.5	93.6	-	768
MS	94.0	93.2	93.5	-	
SG	<b>94.5</b>	93.0	-	<b>94.0</b>	
GS	94.2	93.5	-	93.9	
MG	93.9	-	93.4	93.3	
GM	94.2	-	<b>93.9</b>	93.3	
SMG	94.2	92.2	93.0	93.0	512
MSG	94.4	92.7	93.0	93.8	
GSM	94.0	92.7	93.2	93.0	

Table 5. Recall@1 (%) of combined descriptor, and their individual descriptor on CARS196. Each individual descriptor is an output feature vector of each branch right before the concatenating operation. The combined descriptor is the final feature vector of the proposed framework. We report median values from ten runs.

region of an image contributes to the similarity for each final embedding. Figure 4 shows a visualization of topmost (Recall@1) retrieved image of each configuration on the same query.

As mentioned in [49], the regions of similarity are large in the configuration S, while the configuration M has more

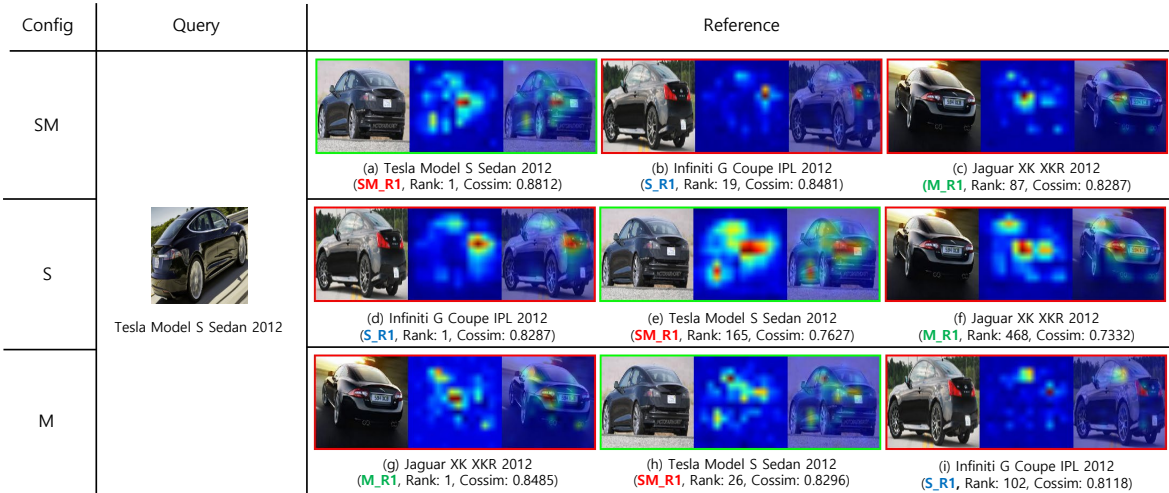


Figure 4. Spatial similarity visualizations on CARS196. Heatmaps show the contribution of each region toward pairwise similarity computation. For each configuration SM, S, and M, we visualize the top 1 retrieved image (a), (d), and (g), respectively, from the same query image. These images are denoted by **SM\_R1**, **S\_R1**, and **M\_R1**. They are used to visualize on different configurations (b, c, e, f, h, i) so that we can see the rank changes among the configurations. The green box indicates that the image is in the same class, while the red box indicates that the image is in a different class. ‘‘Cossim’’ denotes cosine similarity.

focused regions of similarity. The configuration SM seems to have the similarity regions mixed with the configuration S, and M. SPoC tends to see the overall information when it lacks discriminability because they average the high activated outputs by non-active outputs [19]. MAC is preferable to retain the high activation when it is only powerful for sparse features [5]. However, the configuration SM, which has both properties of SPoC, and MAC seems to keep the overall information, and also retain the discriminative regions. This property of the configuration SM pushes up the Figure 4e at the rank of 165 in the configuration S and Figure 4h at the rank of 26 in the configuration M into the rank of 1 as Figure 4a. Following this experiment, combining multiple global descriptors allows the use of different properties of the global descriptors that can help to compute similarity.

#### 4.5. Flexibility of CGD Framework

**Ranking Loss** Table 6 shows that CGD framework can use various ranking losses, such as soft-margin or batch-hard triplet loss [18], HAP2S loss [59], and weighted sampling margin loss [56]. We compare the performance of the configuration S as a baseline for single global descriptor, and SM for multiple global descriptors using these losses. Coefficient  $\alpha$  for HAP2S P loss is set to 10, coefficient  $\sigma$  for HAP2S E loss is set to 0.5, and margin  $\alpha$  and boundary  $\beta$  for margin loss are fixed at 0.1 and 1.2, respectively. In every case, the performance of the configuration SM is better than S, which shows that our framework is flexible in applying various losses.

Config. + Loss	Recall@K (%)			
	1	2	4	8
S + Triplet <sup>†</sup>	93.8 ± 0.2	96.5 ± 0.1	97.8 ± 0.1	98.7 ± 0.1
SM + Triplet <sup>†</sup>	<b>94.3 ± 0.2</b>	<b>96.8 ± 0.2</b>	<b>98.1 ± 0.1</b>	<b>98.9 ± 0.1</b>
S + Triplet <sup>‡</sup>	89.5 ± 0.1	94.2 ± 0.1	96.7 ± 0.1	98.2 ± 0.1
SM + Triplet <sup>‡</sup>	<b>90.4 ± 0.2</b>	<b>94.8 ± 0.2</b>	<b>97.1 ± 0.1</b>	<b>98.5 ± 0.0</b>
S + HAP2S E	93.8 ± 0.3	96.6 ± 0.1	98.0 ± 0.1	98.8 ± 0.1
SM + HAP2S E	<b>94.6 ± 0.1</b>	<b>97.0 ± 0.1</b>	<b>98.2 ± 0.1</b>	<b>98.9 ± 0.0</b>
S + HAP2S P	94.4 ± 0.1	96.9 ± 0.1	<b>98.2 ± 0.1</b>	<b>98.9 ± 0.0</b>
SM + HAP2S P	<b>95.0 ± 0.1</b>	<b>97.2 ± 0.1</b>	<b>98.2 ± 0.1</b>	<b>98.9 ± 0.1</b>
S + Margin	92.8 ± 0.2	95.7 ± 0.1	97.3 ± 0.1	98.3 ± 0.1
SM + Margin	<b>93.9 ± 0.2</b>	<b>96.4 ± 0.1</b>	<b>97.7 ± 0.1</b>	<b>98.6 ± 0.1</b>

Table 6. Recall@K ± std. dev. of the single global descriptor S as a baseline and the combined descriptor SM with various ranking losses on CARS196. <sup>†</sup> denotes the batch-hard triplet, and <sup>‡</sup> denotes the soft-margin hard triplet. We report results over five runs.

**Backbone** Our framework can use different types of CNN backbone. We perform experiments on image retrieval datasets with various CNN backbone: BN-Inception [21], ShuffleNet-v2 [35], ResNet-50 [17], and SE-ResNet-50 [20]. In Table 7a and Table 7b, each value of the same color indicates the same CNN backbone and embedding dimension, which demonstrates that the CGD framework outperforms existing models with the same backbone. Additional experiments with ShuffleNet-v2 presents a reasonable performance even though it is a compact network. Other experiments with SE-ResNet-50 provide the best performance among all as the backbone is very powerful.

**Dataset: Comparison with State-of-the-Art** Finally, we compare our proposed framework with the state-of-the-art

Model	Backbone	Dim	CUB200				CARS196			
			1	2	4	8	1	2	4	8
Facility [38]	BN-Inception	64	48.2	61.4	71.8	81.9	58.1	70.6	80.3	87.8
Proxy-NCA [37]	BN-Inception	64	49.2	61.9	67.9	72.4	73.2	82.4	86.4	88.7
HTL [11]	BN-Inception	512	57.1	68.8	78.7	86.5	81.4	88.0	92.7	95.7
Margin [56]	ResNet-50	128	63.9	75.3	84.4	90.6	86.9	92.7	95.6	97.6
ABE-8 [24]	GoogleNet <sup>†</sup>	512	70.6	79.8	86.9	92.2	93.0	95.9	97.5	98.5
BFE <sup>†</sup> [9]	ResNet-50 <sup>‡</sup>	1536	74.1	83.6	89.8	93.6	94.3	96.8	98.3	98.9
CGD (MG/SG)	BN-Inception	64	<b>61.8</b>	<b>73.2</b>	<b>82.5</b>	<b>89.5</b>	<b>85.7</b>	<b>91.7</b>	<b>95.1</b>	<b>97.3</b>
CGD (MG/SG)	BN-Inception	512	<b>71.9</b>	<b>81.1</b>	<b>88.2</b>	<b>92.9</b>	<b>91.2</b>	<b>95.1</b>	<b>97.0</b>	<b>98.0</b>
CGD (MG/SG)	ResNet-50	128	<b>67.6</b>	<b>78.1</b>	<b>86.3</b>	<b>91.9</b>	<b>90.1</b>	<b>94.3</b>	<b>96.6</b>	<b>98.1</b>
CGD (MG/SG)	ResNet-50 <sup>‡</sup>	1536	<b>76.8</b>	<b>84.8</b>	<b>90.6</b>	<b>94.3</b>	<b>94.7</b>	<b>97.0</b>	<b>98.1</b>	<b>98.9</b>
CGD (MG/SG)	ShuffleNet-v2	1536	66.4	76.5	84.8	91.2	86.1	91.9	94.9	97.1
CGD (MG/SG)	SE-ResNet-50 <sup>‡</sup>	1536	<b>79.2</b>	<b>86.6</b>	<b>92.0</b>	<b>95.1</b>	<b>94.8</b>	<b>97.1</b>	98.2	98.8

(a) Recall@K (%) on CUB200-2011 (cropped) and CARS196 (cropped). CGD (MG/SG) denotes that the configuration MG is used for CUB200-2011 and SG is used for CARS196 on the proposed CGD framework.

Model	Backbone	Dim	SOP				In-shop					
			1	10	100	1000	1	10	20	30	40	50
Facility [38]	BN-Inception	64	67.0	83.7	93.2	-	-	-	-	-	-	-
HTL [11]	BN-Inception	512	74.8	88.3	94.8	98.4	-	-	-	-	-	-
HTL [11]	BN-Inception	128	-	-	-	-	80.9	94.3	95.8	97.2	97.4	97.8
Margin [56]	ResNet-50	128	72.7	86.2	93.8	98.0	-	-	-	-	-	-
ABE-8 [24]	GoogleNet <sup>†</sup>	512	76.3	88.4	94.8	98.2	87.3	96.7	97.9	98.2	98.5	98.7
BFE <sup>†</sup> [9]	ResNet-50 <sup>‡</sup>	1536	83.0	93.3	97.3	99.2	89.1	96.3	97.6	98.5	99.1	-
CGD (SG/GS)	BN-Inception	64	<b>75.6</b>	<b>89.0</b>	<b>95.5</b>	<b>98.6</b>	86.6	96.3	97.4	97.9	98.2	98.4
CGD (SG/ -)	BN-Inception	512	<b>80.5</b>	<b>92.1</b>	<b>96.7</b>	<b>98.9</b>	-	-	-	-	-	-
CGD (- /GS)	BN-Inception	128	-	-	-	-	<b>88.5</b>	<b>97.1</b>	<b>98.0</b>	<b>98.5</b>	<b>98.8</b>	<b>98.9</b>
CGD (SG/GS)	ResNet-50	128	<b>81.0</b>	<b>92.2</b>	<b>96.8</b>	<b>99.1</b>	88.4	97.2	98.1	98.4	98.7	98.8
CGD (SG/GS)	ResNet-50 <sup>‡</sup>	1536	<b>83.9</b>	<b>93.8</b>	<b>97.5</b>	<b>99.2</b>	<b>90.9</b>	<b>98.0</b>	<b>98.7</b>	<b>99.0</b>	<b>99.1</b>	<b>99.2</b>
CGD (SG/GS)	ShuffleNet-v2	1536	78.7	90.9	96.1	98.8	86.1	96.9	97.8	98.4	98.6	98.7
CGD (SG/GS)	SE-ResNet-50 <sup>‡</sup>	1536	<b>84.2</b>	<b>93.9</b>	97.4	<b>99.2</b>	<b>91.9</b>	<b>98.1</b>	<b>98.7</b>	<b>99.0</b>	<b>99.1</b>	<b>99.3</b>

(b) Recall@K (%) on Stanford Online Products and In-shop Clothes. CGD (SG/GS) denotes that the configuration SG is used for Stanford Online Products and GS is used for In-shop Clothes on the proposed CGD framework.

Table 7. Performance comparisons with previous state-of-the-art approaches on image retrieval datasets. For better comparison, values with the same color (purple, blue, green, red) have the same backbone, and embedding dimension (Dim), while bold text indicates the best performance within the same color. <sup>†</sup> denotes 256 input size for inference phase, while the rest use 224 input size. <sup>‡</sup> refers to non-conventional usage.

approaches on four image retrieval datasets in Table 7a and Table 7b. To make a fair comparison, we put an experimental result using the same CNN backbone, input size, and output dimension with other approaches. As each dataset has different properties, we choose the best performing configuration with ResNet-50 on each dataset by following the aforementioned rule in Section 3.4 and perform other experiments with the same configuration. Even though BFE [9] uses a 256 input size, and ours uses a 224 input size, the CGD framework gets higher performance on every dataset. Overall, the CGD framework outperforms all the major benchmarks in the image retrieval tasks with a high margin.

## 5. Conclusion

In this paper, we have introduced a simple but powerful framework called CGD for image retrieval. The CGD framework exploits multiple global descriptors to get an ensemble effect when it can be trained in an end-to-end manner. Moreover, the proposed framework is flexible and expandable by global descriptors, CNN backbones, losses, and datasets. We analyze the effectiveness of combined descriptor quantitatively and qualitatively. Our extensive experiments show that exploiting multiple global descriptors lead to higher performance over the single global descriptor because combined descriptor can manipulate different types of feature properties. Our framework performs the best on all the major image retrieval benchmarks considered.



## References

- [1] Gluoncv: a deep learning toolkit for computer vision. <https://gluon-cv.mxnet.io>. 4
- [2] Google landmark retrieval 2019. <https://www.kaggle.com/c/landmark-retrieval-2019>. 1
- [3] A. Babenko and V. Lempitsky. Aggregating local deep features for image retrieval. In *The IEEE International Conference on Computer Vision (ICCV)*, December 2015. 1, 2
- [4] A. Babenko, A. Slesarev, A. Chigorin, and V. Lempitsky. Neural codes for image retrieval. In *European conference on computer vision*, pages 584–599. Springer, 2014. 1
- [5] Y.-L. Boureau, J. Ponce, and Y. LeCun. A theoretical analysis of feature pooling in visual recognition. In *Proceedings of the 27th international conference on machine learning (ICML-10)*, pages 111–118, 2010. 1, 4, 7
- [6] K. Chen, C. Cui, Y. Du, X. Meng, and H. Ren. 2nd place and 2nd place solution to kaggle landmark recognition and retrieval competition 2019. *arXiv preprint arXiv:1906.03990*, 2019. 1, 4
- [7] L.-C. Chen, G. Papandreou, I. Kokkinos, K. Murphy, and A. L. Yuille. Deeplab: Semantic image segmentation with deep convolutional nets, atrous convolution, and fully connected crfs. *IEEE transactions on pattern analysis and machine intelligence*, 40(4):834–848, 2018. 1
- [8] T. Chen, M. Li, Y. Li, M. Lin, N. Wang, M. Wang, T. Xiao, B. Xu, C. Zhang, and Z. Zhang. Mxnet: A flexible and efficient machine learning library for heterogeneous distributed systems. *arXiv preprint arXiv:1512.01274*, 2015. 4
- [9] Z. Dai, M. Chen, S. Zhu, and P. Tan. Batch feature erasing for person re-identification and beyond. *arXiv preprint arXiv:1811.07130*, 2018. 2, 3, 4, 5, 8
- [10] J. Deng, W. Dong, R. Socher, L.-J. Li, K. Li, and L. Fei-Fei. Imagenet: A large-scale hierarchical image database. 2009. 1, 4
- [11] W. Ge. Deep metric learning with hierarchical triplet loss. In *Proceedings of the European Conference on Computer Vision (ECCV)*, pages 269–285, 2018. 8
- [12] R. Girshick. Fast r-cnn. In *Proceedings of the IEEE international conference on computer vision*, pages 1440–1448, 2015. 1
- [13] A. Gordo, J. Almazán, J. Revaud, and D. Larlus. Deep image retrieval: Learning global representations for image search. In *European Conference on Computer Vision*, pages 241–257. Springer, 2016. 1
- [14] A. Gordo, J. Almazán, J. Revaud, and D. Larlus. End-to-end learning of deep visual representations for image retrieval. *International Journal of Computer Vision*, 124(2):237–254, 2017. 3
- [15] Y. Gu, C. Li, and J. Xie. Attention-aware generalized mean pooling for image retrieval. *arXiv preprint arXiv:1811.00202*, 2018. 2
- [16] C. Guo, G. Pleiss, Y. Sun, and K. Q. Weinberger. On calibration of modern neural networks. In *Proceedings of the 34th International Conference on Machine Learning-Volume 70*, pages 1321–1330. JMLR. org, 2017. 3
- [17] K. He, X. Zhang, S. Ren, and J. Sun. Deep residual learning for image recognition. In *Proceedings of the IEEE conference on computer vision and pattern recognition*, pages 770–778, 2016. 1, 3, 4, 5, 7
- [18] A. Hermans\*, L. Beyer\*, and B. Leibe. In Defense of the Triplet Loss for Person Re-Identification. *arXiv preprint arXiv:1703.07737*, 2017. 3, 7
- [19] T. Hoang, T.-T. Do, D.-K. Le Tan, and N.-M. Cheung. Selective deep convolutional features for image retrieval. In *Proceedings of the 25th ACM international conference on Multimedia*, pages 1600–1608. ACM, 2017. 1, 7
- [20] J. Hu, L. Shen, and G. Sun. Squeeze-and-excitation networks. In *Proceedings of the IEEE conference on computer vision and pattern recognition*, pages 7132–7141, 2018. 4, 7
- [21] S. Ioffe and C. Szegedy. Batch normalization: Accelerating deep network training by reducing internal covariate shift. *arXiv preprint arXiv:1502.03167*, 2015. 3, 4, 7
- [22] Y. Kalantidis, C. Mellina, and S. Osindero. Cross-dimensional weighting for aggregated deep convolutional features. In *European Conference on Computer Vision*, pages 685–701. Springer, 2016. 2
- [23] Y. Ke, R. Sukthankar, et al. Pca-sift: A more distinctive representation for local image descriptors. *CVPR (2)*, 4:506–513, 2004. 1
- [24] W. Kim, B. Goyal, K. Chawla, J. Lee, and K. Kwon. Attention-based ensemble for deep metric learning. In *The European Conference on Computer Vision (ECCV)*, September 2018. 1, 2, 3, 4, 5, 8
- [25] D. P. Kingma and J. Ba. Adam: A method for stochastic optimization. *arXiv preprint arXiv:1412.6980*, 2014. 4
- [26] J. Krause, M. Stark, J. Deng, and L. Fei-Fei. 3d object representations for fine-grained categorization. In *Proceedings of the IEEE International Conference on Computer Vision Workshops*, pages 554–561, 2013. 2, 4
- [27] A. Krizhevsky, I. Sutskever, and G. E. Hinton. Imagenet classification with deep convolutional neural networks. In *Advances in neural information processing systems*, pages 1097–1105, 2012. 1
- [28] W. Li, X. Zhu, and S. Gong. Harmonious attention network for person re-identification. In *CVPR*, volume 1, page 2, 2018. 2
- [29] X. Li, M. Larson, and A. Hanjalic. Pairwise geometric matching for large-scale object retrieval. In *Proceedings of the IEEE Conference on Computer Vision and Pattern Recognition*, pages 5153–5161, 2015. 1
- [30] Y. Li, Y. Xu, J. Wang, Z. Miao, and Y. Zhang. Ms-rmac: Multiscale regional maximum activation of convolutions for image retrieval. *IEEE Signal Processing Letters*, 24(5):609–613, 2017. 2
- [31] Z. Lin, Z. Yang, F. Huang, and J. Chen. Regional maximum activations of convolutions with attention for cross-domain beauty and personal care product retrieval. In *2018 ACM Multimedia Conference on Multimedia Conference*, pages 2073–2077. ACM, 2018. 1, 2, 4
- [32] Z. Liu, P. Luo, S. Qiu, X. Wang, and X. Tang. Deepfashion: Powering robust clothes recognition and retrieval with rich annotations. In *Proceedings of the IEEE conference on*

- computer vision and pattern recognition*, pages 1096–1104, 2016. 2, 4
- [33] J. Long, E. Shelhamer, and T. Darrell. Fully convolutional networks for semantic segmentation. In *Proceedings of the IEEE conference on computer vision and pattern recognition*, pages 3431–3440, 2015. 1
- [34] D. G. Lowe. Distinctive image features from scale-invariant keypoints. *International journal of computer vision*, 60(2):91–110, 2004. 1, 2
- [35] N. Ma, X. Zhang, H.-T. Zheng, and J. Sun. Shufflenet v2: Practical guidelines for efficient cnn architecture design. In *Proceedings of the European Conference on Computer Vision (ECCV)*, pages 116–131, 2018. 3, 4, 7
- [36] A. Mikulík, M. Perdoch, O. Chum, and J. Matas. Learning a fine vocabulary. In *European conference on computer vision*, pages 1–14. Springer, 2010. 1
- [37] Y. Movshovitz-Attias, A. Toshev, T. K. Leung, S. Ioffe, and S. Singh. No fuss distance metric learning using proxies. In *Proceedings of the IEEE International Conference on Computer Vision*, pages 360–368, 2017. 8
- [38] H. Oh Song, S. Jegelka, V. Rathod, and K. Murphy. Deep metric learning via facility location. In *Proceedings of the IEEE Conference on Computer Vision and Pattern Recognition*, pages 5382–5390, 2017. 8
- [39] H. Oh Song, Y. Xiang, S. Jegelka, and S. Savarese. Deep metric learning via lifted structured feature embedding. In *Proceedings of the IEEE Conference on Computer Vision and Pattern Recognition*, pages 4004–4012, 2016. 2, 4
- [40] M. Opitz, H. Possegger, and H. Bischof. Efficient model averaging for deep neural networks. In *Asian Conference on Computer Vision*, pages 205–220. Springer, 2016. 2, 3
- [41] M. Opitz, G. Waltner, H. Possegger, and H. Bischof. Bierboosting independent embeddings robustly. In *International Conference on Computer Vision (ICCV)*, 2017. 1, 2
- [42] K. Ozaki and S. Yokoo. Large-scale landmark retrieval/recognition under a noisy and diverse dataset. *arXiv preprint arXiv:1906.04087*, 2019. 1, 4
- [43] F. Radenović, G. Toliás, and O. Chum. Fine-tuning cnn image retrieval with no human annotation. *IEEE Transactions on Pattern Analysis and Machine Intelligence*, 2018. 1, 2
- [44] J. Redmon, S. Divvala, R. Girshick, and A. Farhadi. You only look once: Unified, real-time object detection. In *Proceedings of the IEEE conference on computer vision and pattern recognition*, pages 779–788, 2016. 1
- [45] S. Ren, K. He, R. Girshick, and J. Sun. Faster r-cnn: Towards real-time object detection with region proposal networks. In *Advances in neural information processing systems*, pages 91–99, 2015. 1
- [46] O. Ronneberger, P. Fischer, and T. Brox. U-net: Convolutional networks for biomedical image segmentation. In *International Conference on Medical image computing and computer-assisted intervention*, pages 234–241. Springer, 2015. 1
- [47] A. Sharif Razavian, H. Azizpour, J. Sullivan, and S. Carlsson. Cnn features off-the-shelf: an astounding baseline for recognition. In *Proceedings of the IEEE conference on computer vision and pattern recognition workshops*, pages 806–813, 2014. 2
- [48] C. Shen, C. Zhou, Z. Jin, W. Chu, R. Jiang, Y. Chen, and X.-S. Hua. Learning feature embedding with strong neural activations for fine-grained retrieval. In *Proceedings of the on Thematic Workshops of ACM Multimedia 2017*, pages 424–432. ACM, 2017. 5
- [49] A. Stylianou, R. Souvenir, and R. Pless. Visualizing deep similarity networks. In *IEEE Winter Conference on Applications of Computer Vision (WACV)*, 2019. 6
- [50] H. Su, C. Li, W. Wei, Q. Wu, and P. Wang. Visual-based product retrieval with multi-task learning and self-attention. 5
- [51] C. Szegedy, V. Vanhoucke, S. Ioffe, J. Shlens, and Z. Wojna. Rethinking the inception architecture for computer vision. In *Proceedings of the IEEE conference on computer vision and pattern recognition*, pages 2818–2826, 2016. 1, 3
- [52] G. Toliás, Y. Avrithis, and H. Jégou. Image search with selective match kernels: aggregation across single and multiple images. *International Journal of Computer Vision*, 116(3):247–261, 2016. 1
- [53] G. Toliás, R. Sicre, and H. Jégou. Particular object retrieval with integral max-pooling of cnn activations. *arXiv preprint arXiv:1511.05879*, 2015. 1, 2, 5
- [54] C. Wah, S. Branson, P. Welinder, P. Perona, and S. Belongie. The caltech-ucsd birds-200-2011 dataset. 2011. 2, 4
- [55] G. Wang, Y. Yuan, X. Chen, J. Li, and X. Zhou. Learning discriminative features with multiple granularities for person re-identification. In *2018 ACM Multimedia Conference*, pages 274–282. ACM, 2018. 3
- [56] C.-Y. Wu, R. Manmatha, A. J. Smola, and P. Krahenbuhl. Sampling matters in deep embedding learning. In *Proceedings of the IEEE International Conference on Computer Vision*, pages 2840–2848, 2017. 7, 8
- [57] X. Wu, G. Irie, K. Hiramatsu, and K. Kashino. Weighted generalized mean pooling for deep image retrieval. In *2018 25th IEEE International Conference on Image Processing (ICIP)*, pages 495–499. IEEE, 2018. 2
- [58] H. Xuan, R. Souvenir, and R. Pless. Deep randomized ensembles for metric learning. In *The European Conference on Computer Vision (ECCV)*, September 2018. 1, 2
- [59] R. Yu, Z. Dou, S. Bai, Z. Zhang, Y. Xu, and X. Bai. Hardware-aware point-to-set deep metric for person re-identification. In *Proceedings of the European Conference on Computer Vision (ECCV)*, pages 188–204, 2018. 7
- [60] A. Zhai and H.-Y. Wu. Making classification competitive for deep metric learning. *arXiv preprint arXiv:1811.12649*, 2018. 4
- [61] X. Zhang, F. X. Yu, S. Karaman, W. Zhang, and S.-F. Chang. Heated-up softmax embedding. In *arXiv preprint arXiv:1809.04157*, 2018. 3
- [62] S. Zhu, X. Dong, and H. Su. Binary ensemble neural network: More bits per network or more networks per bit? *arXiv preprint arXiv:1806.07550*, 2018. 2